JOURNAL OF AIRCRAFT
Vol. 48, No. 2, March–April 2011

Predicting Ejection Velocity of Ejection Seat via Back Propagation Neural Network

Xiao-Dong Mao,* Gui-Ping Lin,† and Jia Yu‡
Beijing University of Aeronautics and Astronautics, 100191 Beijing, People's Republic of China

DOI: 10.2514/1.C031196

The ejection velocity of the escape system, which is a primary parameter of the sequencer control subsystem, determines the parachute shooting time. It is found that, in some certain circumstances, a large error of the measured velocity is generated, which significantly influences the performance of the escape system. In this paper, a method that predicts the ejection velocity by a neural network was presented. Based on the mathematical model, a module simulation solver on the MSC.EASY5 fundamental platform was developed and programmed. According to this solver, considerable ejection conditions that were sufficient to contain all the representative situations in the lifesaving envelope of the escape system were calculated. Then, the relationship between the ejection velocity and other parameters could be obtained from the simulation results. Subsequently, a back propagation neural network was established to fulfill the relationship. Further experimental validation indicated that the error could be accepted in engineering application. Consequently, the method that predicts the ejection velocity via a back propagation neural network was proved to be feasible and would be a useful technology for the escape system.

Nomenclature

a_x	=	acceleration on x-body axis, m/s^2
C_{my}	=	coefficient of aerodynamic moment round y-body axis
C_{xb}	=	coefficient of aerodynamic force on x-body axis
C_{zb}	=	coefficient of aerodynamic force on z-body axis
dt	=	time step
e_H	=	eccentricity of rocket, m
$\boldsymbol{F}$	=	total forces on seat/occupant system, N
F_{aero}	=	aerodynamic force, N
F_H	=	rocket force, N
H	=	ejection height, m
I_{by}	=	moment of inertia round y-body axis, kg · m^2
I_o	=	moment of inertia round point O, kg · m^2
L	=	length of already ejected catapult gun, m
$\boldsymbol{L}_{bmbp}$	=	transformation matrix from plane body-axis system to seat/occupant body-axis system
$\boldsymbol{L}_{bmg}$	=	transformation matrix from global axis system to seat/occupant body-axis system
$\boldsymbol{L}_{bpg}$	=	transformation matrix from global axis system to plane body-axis system
$\boldsymbol{L}_{gb}$	=	transformation matrix from body-axis system to global axis system
L_{ref}	=	reference length of seat/occupant system, m
m	=	mass of seat/occupant system, kg
M_G	=	moment caused by gravity round point O, N · m
M_H	=	moment caused by rocket force round point O, N · m
M_I	=	moment caused by slider impact force round point O, N · m
M_o	=	total moments round point O, N · m
M_P	=	moment caused by lift force round point O, N · m
M_Q	=	moment caused by resistance force round point O, N · m
M_z	=	aerodynamic moment round point O, N · m
r	=	distance from gravity center to point O, m
S_{ref}	=	reference area of seat/occupant system, m^2
V_a	=	airspeed of seat/occupant system, m/s^2
$\boldsymbol{V}k$	=	velocity of seat/occupant system, m/s
x_r	=	value of r projecting on x-body axis, m
z_r	=	value of r projecting on z-body axis, m
α	=	angle of attack, rad
β	=	angle of sideslip, rad
β_H	=	installing angle of rocket, rad
θ	=	pitch angle of seat/occupant system, rad
θ_o	=	angle round point O, rad
ρ	=	density of atmosphere, kg/m^3
ϕ	=	roll angle of seat/occupant system, rad
χ	=	installing angle of seat, rad
ψ	=	yaw angle of seat/occupant system, rad
ω_o	=	angular velocity round point O, rad/s

Subscripts

b	=	body-axis system
g	=	global axis system
p	=	parameters of aircraft
x	=	X direction
y	=	Y direction
z	=	Z direction

I. Introduction

THE ejection seat is the primary equipment to protect the pilot when a military aircraft has an accident. Along with the expanding flight envelope of the aircraft, the escape system must provide the escape capability for a larger scope of the ejection height and velocity. Because of the previous fixed sequence, which does not satisfy the demand of lifesaving in the whole flight envelope, the sequencer control subsystem becomes the crucial and symbolic technology for the third-generation escape system. Several operation modes are predetermined in the sequencer control subsystem for different ejection conditions. When the ejection process starts, the ejection velocity and height are measured with the sensors installed on the seat, and then an operation mode is selected and the parachute opening time is decided [1–4].

Currently, the pitot is used to measure the airspeed on most types of ejection seats. Considerable experiments show that, in some certain circumstances, the actual time of parachute shooting is much earlier than the programmed time. Therefore, insufficient time for the

Presented as Paper 2010-8086 at the AIAA Guidance, Navigation, and Control Conference, Toronto, Ontario, Canada, 2–5 August 2010; received 31 August 2010; revision received 17 September 2010; accepted for publication 22 November 2010.

*Ph.D. Candidate, School of Aeronautic Science and Engineering.
†Professor, School of Aeronautic Science and Engineering.
‡Instructor, School of Aeronautic Science and Engineering.

ejection seat to decelerate would cause an immense deceleration overload on the pilot, which finally leads to a fatal injury or death. The error of the measured velocity is proved to be the main reason of the wrong parachute shooting time. At some special ejection attitudes, such as high angle of attack and high angle of sideslip, which is shown in [5], the velocity measured by the pitot is inaccurate. It is also found during sled tests that fragments of the canopy occasionally jam the pitot, which also leads to a malfunction.

Along with the development of the inertial measurement technology, high precision, small weight, high frequency, and low-cost inertial measurement units are commonly used, even in the escape system. In this paper, a relationship between the acceleration on the x-body axis and the ejection velocity was established beforehand, and then the ejection velocity was calculated in real time by using a back propagation (BP) neural network and the sensed acceleration. This method is proposed to be a backup design or complete substitution of the pitot tube. Comparing with the pitot, the advantages of inertial measurement units involve not using limitations and no interference of the surrounding environment.

II. Method Approach

The accelerometer, as one of the inertial measurement units, was applied in the escape system in this paper. Although the acceleration can be obtained directly, the initial velocity and initial adjustment are two essential requirements to acquire the velocity by integration [6–8]. The velocity is hardly obtained by integration due to the fact that the initial velocity cannot be obtained.

A substitution is a way that establishes the relationship between the acceleration on the x-body axis and the ejection velocity by numerical simulation on the basis of motion characteristics of the seat/occupant system. According to the relationship, a BP neural network was designed and trained. An accelerometer unit was installed at the x-body-axis direction on the ejection seat. Then, given the momentary acceleration when the seat separates from the aircraft, the ejection velocity was finally obtained.

This method needs no large hardware and software modifications on the escape system; the only upgrades are adding an accelerometer unit and a new version program including a neural network solver. The current sequencer control subsystem and control modes are maintained as unchangeable.

III. Simulation Model and Results

A. Coordinate System

The ejection sequence, which is considerably complex, is compartmentalized to four different phases (the catapult phase, the free flight phase, the parachute deploy phase, and the parachute develop phase) according to different forces and motion states. Since what we need is only the momentary acceleration when the seat separates from the aircraft, the catapult phase is the object investigated in this paper.

During the formulation-establishing process, three coordinate systems were used and needed to transform to each other. The three coordinate systems are the global (fixed) axis system, the seat/occupant body-axis system (which is simply called the body-axis system), and the plane body-axis system. The global axis system $oxyz$ attaches to the Earth and does not move with the seat/occupant system. Body orientation and position are measured with respect to this frame. Its origin locates the center of gravity at time zero. The axis ox positively points to the projection of the velocity on the horizontal plane. The axis oy points to the right-facing forward, and the axis oz points vertically downward by the right-hand rule.

The seat/occupant body-axis system $o_2x_2y_2z_2$ is fixed to the seat/occupant system and moves with it, having its origin o_2 at the seat/occupant system center of gravity and identifying with the global axis system at time zero. The o_2z_2 axis is parallel to the catapult centerline and points downward. The o_2x_2 axis is perpendicular to the o_2z_2 axis and points upstream. The o_2y_2 axis is perpendicular to the $o_2x_2z_2$ plane and points to the right of the seat/occupant system. The body-axis system is used to compute forces and moments. The plane body-axis system has the same definition as the seat/occupant body-axis system, except that it is fixed to the aircraft. In the process of calculating, the body-axis system could be translated to the global axis system using the following transformation matrix:

$$\boldsymbol{L}_{gb} = \begin{bmatrix} \cos\theta\cos\psi & \sin\phi\sin\theta\cos\psi - \cos\phi\sin\psi & \cos\phi\sin\theta\cos\psi + \sin\phi\sin\psi \\ \cos\theta\sin\psi & \sin\phi\sin\theta\sin\psi + \cos\phi\cos\psi & \cos\phi\sin\theta\sin\psi - \sin\phi\cos\psi \\ -\sin\theta & \sin\phi\cos\theta & \cos\phi\cos\theta \end{bmatrix} \tag{1}$$

B. Catapult Phase Mathematical Model

The catapult phase begins from the start of the ejection sequence and ends at the time that the seat separates from the aircraft. The ejection seat slides under the constraint of a slider by two pairs of pulleys. The motion has two phases [9–11]. When two pairs of pulleys are both in the slider, the seat would only move along with it and does not rotate. The translational formulation is shown next:

$$\frac{\mathrm{d}\boldsymbol{V}_k}{\mathrm{d}t} = \frac{\boldsymbol{F}}{m} + \boldsymbol{g} \tag{2}$$

Projecting Eq. (2) on the body-axis system and considering that the only effective forces are all in the direction of the o_2z_2 axis, then Eq. (2) can be simplified as

$$\frac{\mathrm{d}V_{k.zb}}{\mathrm{d}t} = \frac{1}{m}F_{zb} + g\cos\phi\cos\theta \tag{3}$$

The total forces that act on the seat/occupant system include the catapult thrust, the gravity of the seat/occupant, the aerodynamic force, and the main rocket impulse. The calculation of the catapult thrust and the rocket impulse came from the experimental data; meanwhile, the wind-tunnel experimental results were used to calculate the aerodynamic force. Because of the uncertain characteristics at the catapult phase, we assumed that at phase one, the seat/occupant system was not affected by the aerodynamic force. At phase two, the aerodynamic force was determined as a whole seat, because 80% of the seat was already in the airstream.

During the period that one pair of pulleys slides out of the slider while the other pair remains in, the seat not only moves along with the slider, but it also rotates around the axis of the remaining pair of pulleys. The rotational formulations are

$$\frac{\mathrm{d}\omega_o}{\mathrm{d}t} = \frac{M_o}{I_o} \tag{4}$$

$$\frac{\mathrm{d}\theta_o}{\mathrm{d}t} = \omega_o \tag{5}$$

$$M_o = M_Z + M_P - M_Q - M_G + M_H + M_I \tag{6}$$

$$\begin{bmatrix} M_Z \\ M_P \\ M_Q \\ M_G \\ M_H \\ M_I \end{bmatrix} = \begin{bmatrix} \frac{1}{2}\rho V_a^2 C_{my} S_{\text{ref}} L_{\text{ref}} \\ \frac{1}{2}\rho V_a^2 C_{\text{zb}} S_{\text{ref}} x_r \\ \frac{1}{2}\rho V_a^2 C_{\text{xb}} S_{\text{ref}} z_r \\ mg(z_r \sin\theta - x_r \cos\phi \cos\theta) \\ F_H\left[e_H + r\cos\left(\beta_H - \arccos\frac{x_r}{r}\right)\right] \\ \frac{3EI_o \sin(-\theta_o)}{L} \end{bmatrix} \tag{7}$$

$$I_o = I_{by} + m \times r^2 \tag{8}$$

By solving Eqs. (1–8), the whole catapult phase can be numerically simulated. From Eq. (3), it was found that the Euler angles of the seat/occupant system were needed in the computational process. The traditional processing method generally considers that the pitch angle of the seat equals the pitch angle of the aircraft plus the seat installing angle, and the roll angles are the same. However, the relationship is inaccurate when the initial roll angle of the aircraft is not zero. This paper obtained a common relationship, which satisfies all the conditions by axis system transformation.

First, we assumed that the vertical symmetry planes of the seat and the aircraft would coincide; therefore, the seat body-axis system could be considered as the plane body-axis system rotates a seat installing angle around the y-body axis. By the conception of coordinate transformation, the transformation matrix from the plane body-axis system to the seat/occupant body-axis system is shown as

$$\boldsymbol{L}_{b_m b_p} = \boldsymbol{L}_y(\chi) = \begin{bmatrix} \cos\chi & 0 & -\sin\chi \\ 0 & 1 & 0 \\ \sin\chi & 0 & \cos\chi \end{bmatrix} \tag{9}$$

Through the matrix transmitting characteristic, the following equations could be obtained:

$$\boldsymbol{L}_{b_m b_p} = \boldsymbol{L}_{b_m g} \boldsymbol{L}_{b_p g}^T \tag{10}$$

$$\boldsymbol{L}_{b_m g} = \begin{bmatrix} \cos\theta\cos\psi & \cos\theta\sin\psi & -\sin\theta \\ \sin\phi\sin\theta\cos\psi - \cos\phi\sin\psi & \sin\phi\sin\theta\sin\psi + \cos\phi\cos\psi & \sin\phi\cos\theta \\ \cos\phi\sin\theta\cos\psi + \sin\phi\sin\psi & \cos\phi\sin\theta\sin\psi - \sin\phi\cos\psi & \cos\phi\cos\theta \end{bmatrix} \tag{11}$$

The matrix of $\boldsymbol{L}_{b_p g}$ can be obtained by substituting the Euler angles of the aircraft into Eq. (11). Connecting Eqs. (9) and (10), comparing the corresponding items, the final relationship between the aircraft Euler angles and the seat/occupant Euler angles is shown, as in Eq. (12):

$$\begin{bmatrix} \psi \\ \theta \\ \phi \end{bmatrix} = \begin{bmatrix} \arctan\frac{\tan\psi_p\cos\theta_p - \cos\phi_p\tan\chi\tan\phi_p(1+\tan\psi_p)}{\cos\theta_p + D(\tan\psi_p - \cos\theta_p)} \\ \arcsin(\sin\theta_p\cos\chi + \cos\theta_p\cos\phi_p\sin\chi) \\ \arctan\frac{\sin\phi_p}{-\tan\theta_p\sin\chi + \cos\phi_p\cos\chi} \end{bmatrix} \tag{12}$$

C. Simulation Model Based on MSC.EASY5 Platform

The escape system is a complex system that involves many subsystems, and each subsystem performs a unique function at the ejection sequence. According to this feature and the conception of modularization, a solver on the MSC.EASY5 fundamental platform, including different modules based on the physical characteristics, was developed and programmed [12,13]. The modules consist of the seat/occupant motion module, the aircraft module, the catapult module, the aerodynamic force module, the main rocket module, the seat structure parameters module, the data output interface module, and the outer data interface module. After the data flowpaths are bridged, the time history of the parameters transferred among these modules simulates the realistic physical process. Figure 1 shows the schematic diagram of the module partition and the data flowpaths.

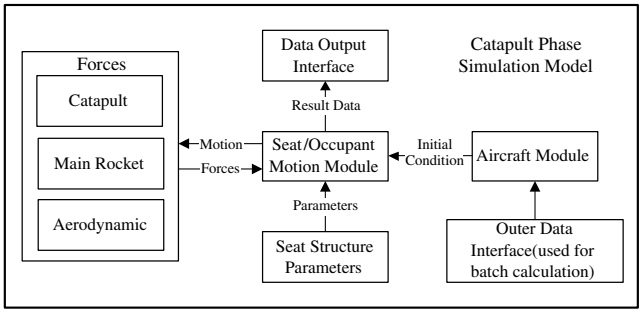

Fig. 1 MSC.EASY5 simulation model.

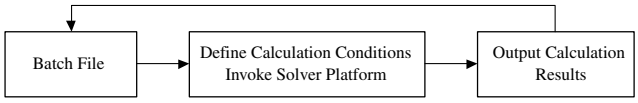

Fig. 2 Flowchart of calculation.

Since numerous ejection conditions need to be calculated, the batch command method was applied to implement fully automatic processing. The definition of calculating conditions and solver platform invoking were all accomplished by the batch file; the flowchart of the calculation is shown as Fig. 2.

D. Analysis of Influence Factors on Acceleration

Based on Newton's second law, the acceleration on the x-body axis can be written as

$$a_x = \frac{F_{\text{aero.xb}} + F_{H.\text{xb}} + G_{\text{xb}}}{m} = \frac{f(Ma, \alpha, \beta) + F_{H.\text{xb}}}{m} - \cos\phi\sin\theta \tag{13}$$

From Eq. (13), it can be found that the acceleration refers to the aerodynamic force, the rocket impulse, the seat/occupant mass, and the Euler angles. Ignoring the seat's unchangeable parameters, such as the catapult impulse and the installing angle of the seat, the influence factors on the acceleration are the ejection height, the ejection velocity, the mass of the seat/occupant system, the eccentricity of the main rocket, the pitch angle of the plane, the roll angle of the plane, and the roll angular rate of the plane. The acceleration can be ultimately expressed as a function of seven independent variables, shown as

$$a_x = f(H, V, m, e_H, \theta_P, \phi_P, \omega_P) \tag{14}$$

The influence principle of the rocket eccentricity is that different eccentricities generate different moments, which result in different deformations of the catapult. Therefore, the direction of the velocity and, finally, the value of the acceleration would be different. The

Table 1 Influence of rocket eccentricity

Rocket eccentricity, mm	Acceleration, m/s^2
10	−42.4161
5	−42.4149
0	−42.4137
5	−42.4172
10	−42.4184

influence of the rocket eccentricity (fix the other parameters) is calculated by the simulation model and listed in Table 1.

The results shown in Table 1 indicate that the effect of the rocket eccentricity is extremely small, so the ignorance is reasonable. Since the disadvantage attitude angles are not considered, as the operation mode parameters of the third-generation escape system and the seat have no capability of sensing attitude angles, the attitude variables are also neglected in this paper. Hence, Eq. (14) is simplified as Eq. (15):

$$a_x = f(H, V, m) \tag{15}$$

E. Simulation Results

According to Eq. (15), various conditions sufficient to contain all the representative ejection conditions in the envelope of the escape system were calculated, and the results were obtained in tabulation format. To observe the relationship between the acceleration and the ejection velocities, curves of the acceleration versus the ejection velocities for typical ejection heights and typical seat/occupant masses are displayed in Fig. 3.

From Fig. 3a, it can be seen that, as the ejection velocity rises, the acceleration decreases; in other words, the corresponding deceleration increases. At the range of low ejection velocities, the acceleration is positive. On the contrary, at the high-velocity range, the acceleration is negative. When the velocity is close to 700 kph, the acceleration is close to zero. The acceleration increases as the ejection height increases at the same ejection velocity. The reason is because the faster the ejection velocity, the larger the aerodynamic resistance force. If the main rocket impulse is greater than the aerodynamic force, the acceleration is positive; otherwise, it is negative. At the higher ejection height, the atmosphere density becomes lower, so the same velocity generates a smaller aerodynamic force.

As shown in Fig. 3b, when the mass grows larger, the curve becomes more and more steep. The reason can be easily interpreted by Eq. (13). If the total force is the same, the larger the mass, the smaller the absolute acceleration value.

Ultimately, the relationship between the acceleration and the ejection velocities was established by a simulation method. Then, the next problem is implementing the mapping from the input parameters to the ejection velocity, which will be discussed in the next section.

IV. Back Propagation Neural Network Implementation

A. Neural Network Establishment

From Eq. (15), we can get the deformation as

$$V = f_1(a_x, H, m) \tag{16}$$

Equation (16) indicates that the velocity is a function of three independent variables, but it is difficult to get the exact function formula in practice. The relationship among the velocity and the preceding three variables, obtained in the previous section, is in a tabular format, which is not convenient to use directly. Neither interpolation nor function fitting are ideal methods due to the unpredictable errors.

An artificial neural network is a complicated network system composed of considerable fundamental elements called neurons. It is used for parallel processing and nonlinear transformation by simulating the human brain neural processing mode. Research on the neural network started in the 1940s; because of its powerful study ability, parallel computation capability, and convenient characteristic of implementing nonlinear mapping, it has been widely applied in many areas and become one of the most interesting and charming research subjects in the artificial intelligence domain [14,15].

We took the advantage of the neural network in order to obtain a nonlinear mapping from the three independent variables to the ejection velocity. The usage of the neural network system can be comprehended as the fitting function f_1 in Eq. (16). In this paper, the MATLAB neural network toolbox was used to establish the network system. A BP neural network containing three layers was set up. The numbers of layers and nodes depends on the number of parameters and the required precision. The first layer is an input layer, and the other two are network layers. The input vector has three dimensions consisting of the acceleration, the ejection height, and the seat/occupant mass. The output parameter is the demanded ejection velocity. Meanwhile, Levenberg–Marquardt is selected as the training arithmetic for its features of high convergence speed and wonderful precision. The training samples coming from the simulation results are sufficient to contain all the representative ejection conditions in the envelope of the escape system.

B. Results

During the training process, the largest error departing from the sample points is 5.77 kph. Once the training is done, three points

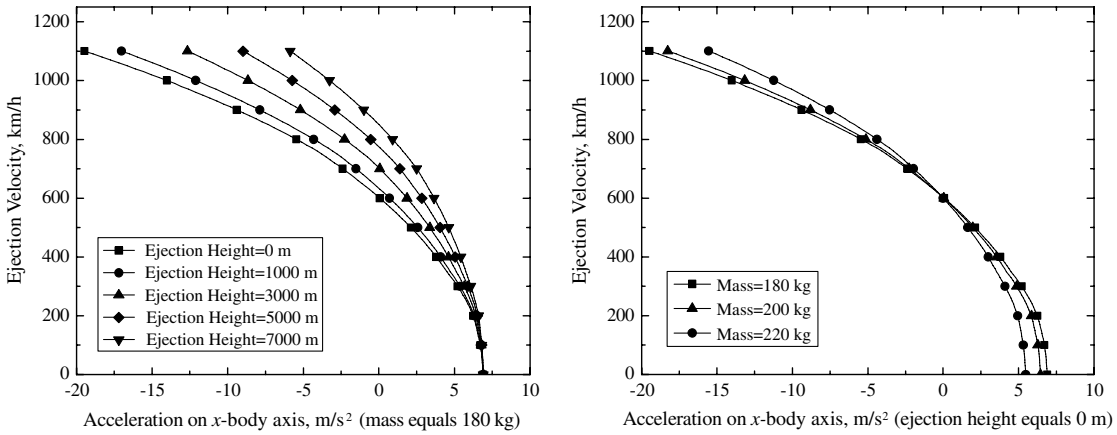

a) Different ejection heights **b) Different seat/occupant masses**

Fig. 3 Relationship of acceleration versus ejection velocity at various heights and masses.

Table 2 Neural network testing results

No.	Ejection height, m	Acceleration, m/s^2	Actual ejection velocity, $km \cdot h^{-1}$	Neural network processing result, $km \cdot h^{-1}$	Error, $km \cdot h^{-1}$
1	432	50.65200	267	268.9392	1.9392
2	3589	4.96714	694	696.2456	2.2456
3	6983	−35.21590	1024	1018.0000	6.0000

Table 3 Network processing results comparing with experimental data

Experimental ejection velocity, $km \cdot h^{-1}$	Acceleration, m/s^2	Neural network processing result, $km \cdot h^{-1}$	Error, $km \cdot h^{-1}$
0	76.6184	0	0
100.0	65.1660	72	28.0
397.8	40.1638	365	32.8
504.0	6.6941	570	66.0
536.0	12.8841	535	1.0
802.0	−76.6600	870	68.0
1081.0	−147.5111	1080	1.0
1107.0	−183.6632	1110	3.0
1147.0	−174.5934	1140	7.0

which are not in the bound of the sample points are selected to test the already built network, the results are listed below in Table 2.

As can be seen from the data in Table 2, the neural network processing result meets the actual ejection velocity well and the error caused by the neural network calculation can be absolutely accepted. If less error is expected, it can be easily acquired by adjusting the structure of the network. Thus, predicting the ejection velocity by a neural network is proved to be feasible.

C. Experiment Validation

Finally, the already trained neural network should be verified by rocket sled test data. There are nine sled tests covering all of the velocity scope. The actual experimental height, the seat/occupant mass, and the sensed acceleration are conducted as the input vector to the neural network. The processing result compared with the actual ejection velocity is listed in Table 3.

From Table 3, it can be seen that, at the high ejection velocity range, the processing result meets the experimental result very well, because at these conditions, the aerodynamic force is the primary force acting on the seat/occupant system, which effectively decreases the influence of the other unpredictable factors. On the other hand, at the middle and low ejection velocity ranges, the error becomes greater because of effects such as the uncertainties of the catapult and the rocket impulse. In addition, the simplification of the aerodynamic force in the catapult phase mathematical model introduces some error. However, the error in total is absolutely acceptable for engineering applications.

V. Conclusions

The method of predicting the ejection velocity by a BP neural network has proved to be feasible. Depending on the already trained neural network, it is convenient to obtain the velocity by just inputting the other three parameters, which are the acceleration on the x-body axis, the ejection height, and the seat/occupant mass. Comparison between the neural network processing result and the experimental result indicates that the error meets the requirement for engineering application. Further research that establishes a complete relationship involving the initial disadvantage attitude angles and a revising neural network structure in order to fit all the ejection conditions needs to be done.

Acknowledgment

The rocket sled test data were provided by the China Aviation Life Support Institute.

References

[1] Zhou, F., "Measures to Improve the Successfulness of Ejection Escaping in the Low Altitude Positions," *Aeronautic Science and Technology*, Vol. 5, No. 6, 1998, pp. 18–20.

[2] Li, R., "Exploration of K36-3.5 Ejection Seat Operation Model," *China Aeronautical and Astronautical Life Support*, Vol. 26, No. 3, 2004, pp. 1–6.

[3] Li, R., "Performance Analysis of K36-3.5 Ejection Seat," *China Aeronautical and Astronautical Life Support*, Vol. 28, No. 1, 2005, pp. 1–6.

[4] Zhu, J. H., *Inertia Navigation*, National Defense Industry Press, Beijing, PRC, 2008, pp. 82–125.

[5] Chen, Y. B., and Zhong, B., *Principle of Inertia Navigation*, National Defense Industry Press, Beijing, PRC, 2007, Chap. 2.

[6] *Handbook of Aircraft Design*, Vol. 15, Aviation Industry Press, Chief Edition Committee, Beijing, PRC, 1999, pp. 458–474.

[7] Zhang, H. B., *Aircraft Escape System*, Beijing Univ. of Aeronautics and Astronautics Press, Beijing, PRC, 1990, Chap. 4.

[8] Zhou, K. L., and Kang, L. H., *Neural Network Model and MATLAB Simulating Program Design*, Tinghua Univ. Press, Beijing, PRC, 2005, Chap. 5.

[9] Ge, Z. X., and Sun, Z. Q., *Theory Neural Network and MATLAB R2007 Implementation*, Publishing House of Electronics Industry, Beijing, PRC, 2007, Chap. 4.

[10] McCauley, D., "Future Advanced Sequencer Technology (FAST)," *SAFE Association 39th Annual Symposium*, Survival and Flight Equipment Assoc., Creswell, OR, Sept. 2001, pp. 95–110.

[11] Yu, J., and Lin, G. P., "Numerical Simulation of Ejection Seat Performance at Adverse Attitude Condition," *SAFE Association 45th Annual Symposium*, Survival and Flight Equipment Assoc., Creswell, OR, Oct. 2007, pp. 116–124.

[12] Harrington, P. B., "Aviation Structural Mechanic E2," Naval Education and Training Professional Development and Technology Center, NAVCDTRA 14020, Pensacola, FL, Aug. 1989.

[13] Glen, B., Nortron, B., and Lingard, J. S., "Inertially Controlled Recovery System (ICRS)," AIAA Paper 1999-1718, 1999.

[14] Ma, D., Obergfell, L., Rizer, A., and Rogers, L., "Biodynamic Modeling and Simulation of the Ejection Seat/Occupant System," U.S. Air Force Research Lab., AFRL-HE-WP-TR-2000-0080, Wright-Patterson AFB, OH, 2000.

[15] Elson, M., and Lingard, J. S., "Object Orientated Ejection Seat Model," AIAA Paper 1997-1548, 1997.